

High dynamic range head-up displays

JUNYU ZOU,^{1,2} EN-LIN HSIANG,^{1,2} TAO ZHAN,¹  KUN YIN,¹ ZIQIAN HE,¹ AND SHIN-TSON WU^{1,*} 

¹College of Optics and Photonics, University of Central Florida, Orlando, FL 32816, USA

²These authors contributed equally to this work

*swu@creol.ucf.edu

Abstract: We demonstrate a full-color high dynamic range head-up display (HUD) based on a polarization selective optical combiner, which is a three-layer cholesteric liquid crystal (CLC) film. Such a CLC film has three reflection bands corresponding to the three primary colors. A key component in our HUD system is a polarization modulation layer (PML) consisting of a twisted-nematic LC polarizer sandwiched by two quarter-wave plates. This spatially switchable PML generates opposite polarization states for the displayed image and its background area. Thus, this optical combiner reflects the displayed image to the observer and transmits the background noise, making the black state darker. Furthermore, by matching the reflection spectra of the optical combiner with the colors of the display panel, the bright state gets brighter. Therefore, both bright state and dark state are improved simultaneously. Our experimental results show that the dark state of the new HUD is lowered by 3x and bright state is boosted by 2.5x. By applying antireflection coating to the optical components and optimizing the degree of polarization, our simulation results indicate that the dynamic range can be improved by ~50x (17 dB). Potential applications of the proposed HUDs for improving the driver's safety are foreseeable.

© 2020 Optical Society of America under the terms of the [OSA Open Access Publishing Agreement](#)

1. Introduction

The concept of the head-up display (HUD) was first demonstrated in aircrafts as early as 1960s [1]. It took more than two decades of intensive development efforts to penetrate to the automobile industry [2], enabling the driver to focus on the road conditions. Recently, HUD has been widely implemented in vehicles as an advanced driver assistance system [3,4].

The optical structure of a commercial HUD usually consists of three parts: light engine, folding optics, and optical combiner (OC) [5,6]. At present, many HUDs use liquid crystal display (LCD) as the light engine because of its low cost, good temperature stability, and long lifetime. However, the major shortcoming of LCD is its relatively low contrast ratio ($CR \approx 2000:1$) due to the depolarization effects of the employed LC and color filters, which leads to a noticeable light leakage in the dark state [7]. As a result, the image of the LCD looks like a transparent postcard emerging in front of the driver. Figure 1(a) shows a photo of the “postcard effect” [8] from a commercial aftermarket HUD. This effect may distract the driver's attention and raise safety concerns. As for the bright state, the strong ambient light and reflection of the display panel could washout the displayed information. Many States in the USA set specific regulations that the ambient light transmittance should be higher than 70%, which means the optical combiner reflectance of the display light toward the driver is below 30%. An inadequate brightness of the perceived image would lead to a low ambient contrast ratio (ACR); that means the image could be washed out by the environment light [9] as Fig. 1(b) shows. To provide the driver with fast recognition, ACR should be larger than 10:1. If $ACR < 3:1$, the driver can hardly recognize the displayed information and it raises safety alert [10]. Therefore, both dark state and bright state of the HUDs should be improved. In other words, HUDs with high dynamic range (HDR) are highly desirable.

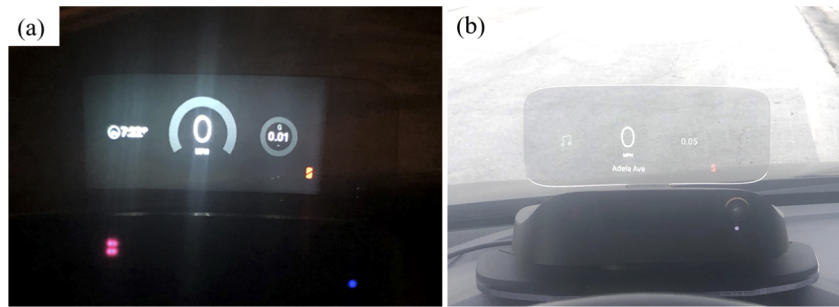


Fig. 1. Problems in current commercial HUD: (a) postcard effect and (b) image washout.

To achieve HDR, we can enhance the HUD performance from light engine or from optical combiner. Currently, digital light processing (DLP) and laser scanned micro-electromechanical systems (MEMS) are two strong contenders for the image generation unit of HUD [11–13]. Digital micromirror device (DMD) is a critical component in the DLP-based HUD system. A DMD consists of millions of micro-mirrors that can be switched individually between two states by the applied voltage. To generate a bright image, the incident light is reflected by the micro-mirror toward the optical system. Although DMD is a bistable device, grayscale can be generated by the pulse width modulation method. To obtain dark state, the incident light is reflected off the projection lens and absorbed by the surrounding black paint. On the other hand, in the laser scanning MEMS projection system, the image content is written by the RGB lasers, which scan over the screen through a two-dimensional MEMS mirror. Both approaches can provide HDR images for HUD applications, however, the complicated driving system and high cost remain to be overcome before widespread applications can take place.

Other potential image generation units like OLED, mini-LED backlit LCD, and micro-LED have their pros and cons. OLED exhibits an excellent dark state and thin form factor, but the high temperature inside a vehicle and high peak luminance (>2000 nits) requirement for HUDs could lead to serious burn-in and degraded lifetime [14]. Mini-LED backlit LCD can achieve a reasonably high luminance and long lifetime, but the halo effect could distract the driver's attention. The halo effect can be suppressed by using more mini-LEDs and local dimming zones [15], but to drive thousands of mini-LEDs the IC cost is relatively high, and the driving method is complex. Micro-LED would be an attractive solution, but the manufacturing yield, defect repairs, and cost issue remain to be overcome [16,17].

Modifying the optical combiner is another promising approach to enhance the dynamic range. Here we define T as the ambient light transmittance through the optical combiner, and R as the reflectance of the optical combiner to the display light. For an ideal optical combiner, it should transmit all the ambient light and reflect all the display light, i.e. $R + T = 200\%$. In a conventional optical combiner, the transmittance of ambient light and the reflectance of display light sums up to 100% ($R + T = 100\%$), assuming the absorption is negligible. However, if the bright state of the HUD is improved, and the transmittance of the optical combiner keeps higher than 70%, then $R + T$ could exceed 100%. To realize this special advantage, the display light should exhibit different characteristics from the ambient light.

The first difference is wavelength spectrum. The spectrum of ambient light is usually broadband and continuous, similar to D65 (white light), in the visible spectrum. However, the display light usually consists of three primary colors (red, green, and blue, RGB). Based on this difference, holographic film would be an attractive candidate for the optical combiner because of its narrow and sharp reflection band [18]. Thus, if the OC's reflection bands match the display's primary colors, then more light from the display panel will be reflected toward the observer. In the

meantime, more ambient light will transmit through the OC because it only reflects the RGB bands and transmits the remaining visible light. With the help of holographic film, the value of $R + T$ can reach as high as 170% [19], but only for monochromatic displays.

The second difference is the polarization state. The ambient light is usually unpolarized or with a low degree of polarization. However, the display panel (LCD or OLED) emits polarized light [20]. Based on this difference, a polarization selective OC has been designed for HUD [21,22] to introduce different reflectance for display light and ambient light. In contrast, a conventional OC exhibits same transmittance (e.g. 70%) for the randomly polarized ambient light and left-handed circularly polarized (LCP) display light, as Fig. 2(a) shows. In this scenario, $R + T \approx 100\%$. If the polarization selective OC reflects LCP by 60% but transmits right-handed circularly polarized (RCP) by 100%, as Fig. 2(b) depicts, then the reflectance of display light ($R=60\%$) can be improved by 2x in comparison with conventional optical combiner ($R=30\%$). Under such conditions, $R=60\%$ and $T=70\%$, and $R + T \approx 130\%$.

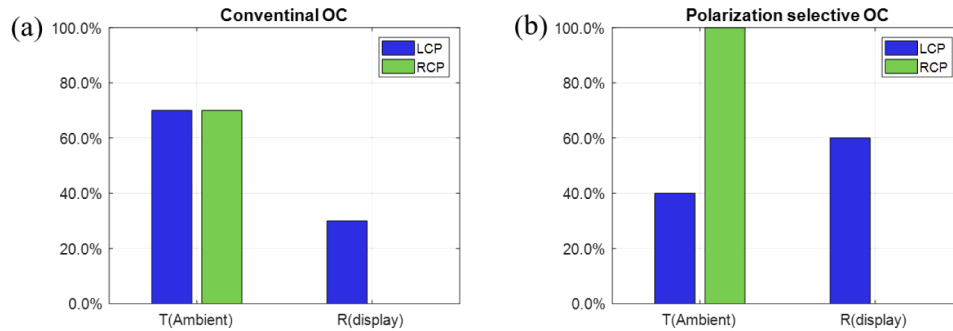


Fig. 2. Ambient light transmittance and display light reflectance of (a) conventional OC and (b) polarization selective OC based on LCP and RCP.

In this paper, we demonstrate an HDR HUD system based on a polarization selective OC, which consists of three cholesteric liquid crystal (CLC) films [23,24]. Such a CLC film reflects only one circular polarization in the desired RGB bands. Moreover, a polarization modulation layer (PML) is employed to modulate the polarization state of each pixel on the LCD, such that the polarization states of dark pixels and bright pixels can be distinguished. The light emitted from bright pixels is reflected by the OC, while that from dark pixels is transmitted. With this design, both bright and dark states of the HUD are improved. With the help of polarization selective OC, the ambient light transmittance remains relatively high.

2. System configuration

Figure 3(a) shows the system configuration. Two quarter-wave plates (QWP) and a 90° twisted nematic (TN) panel are placed between the projection lens and display to serve as the PML. The evolution of polarization states from the display to the projection lens is illustrated in Fig. 3(b). Let us assume the display panel emits LCP light, the first QWP converts the LCP light to linear polarization. The TN panel serves as a switchable polarization rotator [25,26]. For those TN pixels in the voltage-off state, they rotate the incoming linearly polarized light by 90°, as shown in the right part of Fig. 3(b). Then, the second QWP changes the linearly polarized light to RCP, which in turn will transmit through our CLC based OC. For those TN pixels with a high voltage, the LC directors will be reoriented along the direction of light propagation. As a result, the incoming linearly polarized light experiences no phase retardation effect and will not be affected, as shown in the left part of Fig. 3(b), so that the outgoing light will be LCP.

To illustrate the basic operation principle of our system, in experiment we use an iPhone 8 as the display panel and a 7" TN panel (resolution 800 × 480 but without polarizers) sandwiched

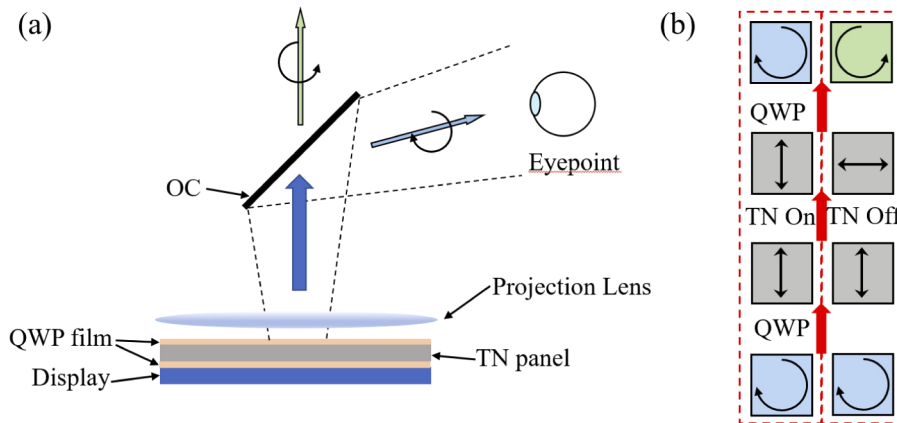


Fig. 3. (a) Schematic diagram of the HUD system, and (b) polarization state evolution in the polarization modulation layer. Here, we assume the display panel emits LCP light, while the OC reflects LCP and transmits RCP.

between two QWPs as the PML, as Fig. 3(a) depicts. For convenience of discussion, let us assume the display light from iPhone 8 is LCP. First, we use iPhone 8 to generate colored UCF patterns. Then, we apply a voltage (≈ 5 V) to those corresponding TN pixels to retain the polarization state (LCP) of UCF as the left part of Fig. 3(b) indicates. The remaining pixels of the TN panel are at $V=0$ so that the outgoing light passing through this region will be RCP. Due to the polarization selectivity of our optical combiner, the light with UCF characters (LCP) will be reflected toward the observer's eye, as Fig. 3(a) shows. While the remaining light with RCP will pass through the OC, making the black area even darker.

3. Experiment

3.1. CLC optical combiner

In the proposed system, the main component is the polarization selective optical combiner, which is a three-layer CLC film. Such a CLC film exhibits helical structure; it reflects the circularly polarized light with the same handedness, (e.g., LCP), but transmits the opposite polarization (RCP) [27]. The central wavelength (λ_o) of the Bragg reflection is jointly determined by the CLC helical pitch length (p) and average refractive index (n) of the employed LC material as $\lambda_o = p \cdot n$ [27].

In experiment, we used RM257 (from LC Matter) as LC monomer, whose average refractive index is 1.508 and birefringence is 0.152, 0.161, 0.176 at 630 nm, 530 nm, 450 nm, respectively. S5011 (from HCCH) was chiral dopant, which made the LC directors rotating along the helical axis. By adjusting the concentration of chiral dopant, the CLC pitch length can be changed, and the central wavelength of Bragg reflection can be tailored to a desired value. The CLC film has three layers, and each layer has the central wavelength locates at red, green, and blue spectrum, respectively. In our design, the helical pitch length for the RGB layers is around 417 nm, 351 nm and 298 nm, respectively, and the thickness of each layer is restricted to ~ 5 helical pitches by controlling the ratio of solute and solvent in the CLC solution, and the speed of spin-coating, so that the reflection peak will not be too high ($\sim 80\%$) [27] in order to let 70% ambient light transmit through. The blue and green CLC layers were spin-coated on two separate 2-inch glass substrates, and the red one was spin-coated on top of the blue one as Fig. 4(a) shows. Then the two substrates were laminated together to form a three-layer CLC polymer film, which was robust and thermoresistant. The reason we fabricated blue and red CLC layers on the same substrate

is explained as follows. If we fabricated two layers with close central wavelength together (e.g. blue and green, or green and red), then the two reflection bands will merge into one, because RM257 has a relatively high birefringence and the reflection band is broad. Since the OC is inclined at around 45° , the reflection spectrum with LCP input at 45° was measured and results plotted in Fig. 4(b) where three reflection bands at RGB primary wavelengths can be observed. The fabricated OC also shows a reasonable transmission spectrum with an unpolarized light input at 45° , as shown in Fig. 4(c). The spectrums were measured by a white light spectrometer (Ocean Optics HG2000CG) with a halogen lamp.

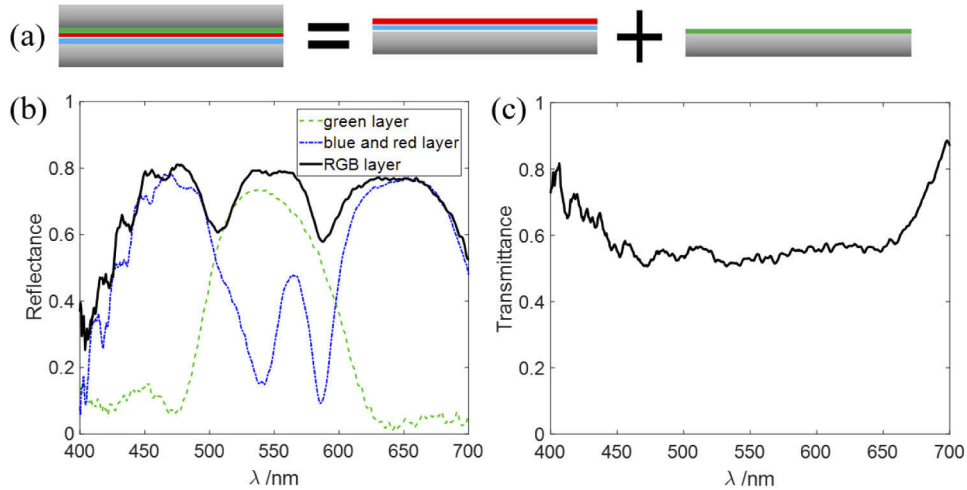


Fig. 4. (a) Three-layer CLC film structure, (b) measured reflection spectrum (normalized to a glass substrate) of the green CLC layer, blue & red CLC layers, and three-layer RGB CLC film with LCP input, and (c) measured transmission spectrum of the three-layer CLC film with an unpolarized light, which is also normalized to a glass substrate.

3.2. Results

As Fig. 3(a) shows, the optical combiner is inclined at 45° from the horizontal plane so that the observer can see the image in horizontal direction. The experimental setup in a bright environment (~ 500 lux) is shown in Fig. 5(a), in which the device is illuminated by a fluorescent tube with color temperature at ~ 6500 K. Figure 5(b) is a control group, whose OC is a 2-inch glass substrate without any film. By comparing the performance of these two optical combiners, the image washout in Fig. 5(b) is serious because of the relatively low reflectance in the glass-air interface, which is around 10% at 45° . The display we used is a LCD panel from iPhone 8, whose original emitting spectrum and the spectrum after the polarization selective OC are plotted in Fig. 6(a). Through integrating the area covered by the red line and then divided by the area covered by the blue line in Fig. 6(a), we find our CLC-based optical combiner reflects $\sim 74.5\%$ of the light from display panel. In comparison, we also tested the commercial HUD we have in our lab (the one we used in Fig. 1), and found its reflectance is only 30%. Thus, the brightness gain is ~ 2.5 x, which helps to enhance the ambient contrast ratio. Meanwhile, our OC exhibits $\sim 66.2\%$ transmittance as shown in Fig. 6(b), which is comparable to the commercial one ($\sim 70\%$). Later, we will show a new optical combiner design with $T \sim 78.9\%$ using a low birefringence reactive mesogen.

Next, we tested the performance of our polarization selective optical combiner in dark environment. In order to show the effect of PML, we took two photos of the HUD from the observer's position shown in Fig. 3(a). Results are depicted in Fig. 7(a) and Fig. 7(b).

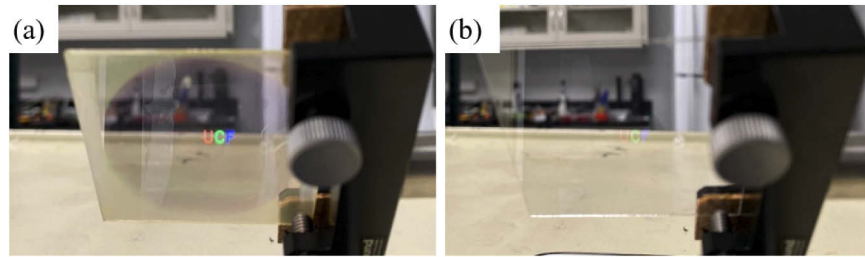


Fig. 5. Image results of HUD system with (a) CLC film-based OC, and (b) glass OC in a bright environment (~500 lux).

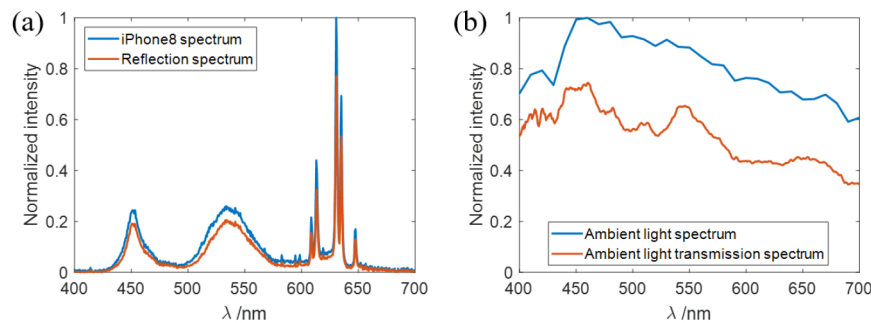


Fig. 6. (a) Original and reflection spectrum of the display panel, and (b) original and transmission spectrum of ambient light. Light source: iPhone 8.

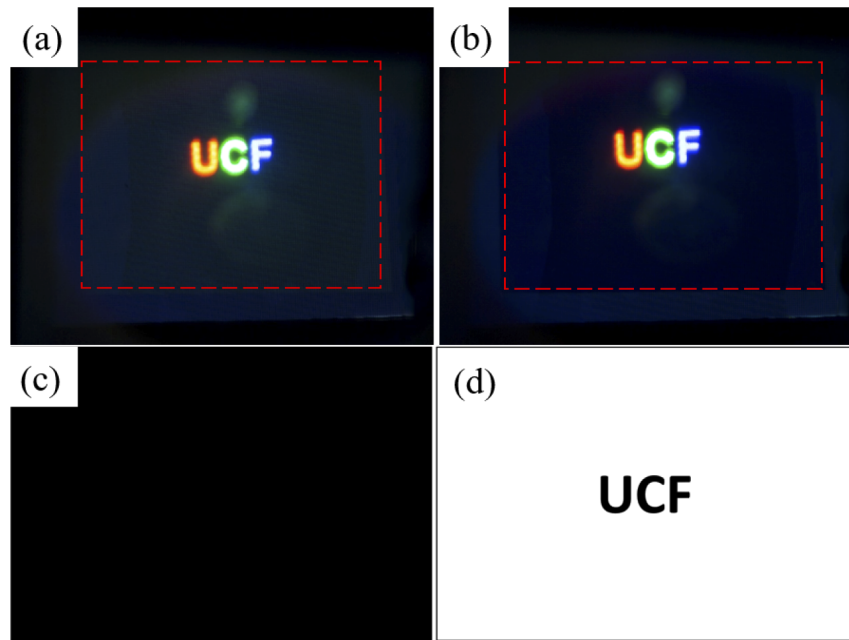


Fig. 7. Imaging results of proposed HUD system when the PML is (a) off and (b) on in dark environment (dotted lines stand for the effective area of PML), and the signal input to the TN panel when the PML is (c) off and (d) on. ([Visualization 1](#) shows the recorded video. It is recommended to watch the video in dark ambient so that the contrast ratio improvement is more obvious than those photos (a) and (b) taken by a camera.)

In Fig. 7(a), the input signal to the TN panel is a black image as Fig. 7(c) shows. All the pixels in the TN panel are with 5 V so that the display light after passing through the PML remains LCP, which in turn is reflected by the optical combiner toward the observer. Thus, the imperfect dark state from iPhone 8 (CR \approx 1400:1) degrades the image contrast ratio. On the other hand, in Fig. 7(b), the input signal to the TN panel is a black and white “UCF” pattern as Fig. 7(d) shows, in which the UCF pattern matches the position of colored UCF pattern on iPhone 8 (resolution 1334 \times 750). Therefore, only those pixels in the TN panel corresponding to UCF pattern are activated (5 V), while the remaining pixels remain off (V=0). As a result, the UCF pattern preserves LCP and is reflected by the optical combiner, while the background area (RCP) transmits through. Therefore, the background light level is reduced and the black state gets darker, as Fig. 7(b) shows. According to our measurement [measured by a photoreceiver (New Focus 2031) and a luminance meter (Konica Minolta LS-110)], with the help of PML the dark state is suppressed by 3x, i.e. contrast ratio is 3x higher.

Here we briefly summarize our experimental results: the bright state is improved by 2.5x and the dark state is enhanced by 3x, resulting in a 7.5x total improvement. The dynamic range (unit: decibel) is related to CR as $10 \times \log(\text{CR})$. Thus, the dynamic range of our iPhone 8 based HUD is improved from $10 \times [\log(1400)]$, which is 31.46 dB, to $10 \times [\log(7.5 \times 1400)]$, which is 40.21 dB. The net gain is 8.75 dB. During calculation, we find the dynamic range improvement is independent of the display panel’s CR.

In principle, all the RCP should transmit through the CLC optical combiner if only Bragg reflection is considered. However, we still need to consider the Fresnel reflection at the air-glass interface, which accounts for 5.3% at 45° incidence angle, according to the Fresnel equations. Moreover, due to the small scattering originated from the TN panel, the display light is no longer completely polarized after passing through the PML. Figure 8 shows the simulated relationship between the degree of polarization and contrast ratio improvement for the dark state. In experiment, the degree of polarization is 88% at $\lambda=532$ nm. From Fig. 8(a), the CR improvement for the dark state is \sim 6x in simulation and 5.6x in experiment. The agreement is good. If the Fresnel reflection is reduced to 1.2% by antireflection coating on the surface, then the CR improvement for the dark state can reach 11.3x [Fig. 8(b)]. Furthermore, when the degree of polarization increases to 95%, the CR improvement for the dark state is nearly 20x. Combining with the bright state improvement, the total CR improvement of system is 50x, which corresponds to 17 dB dynamic range enhancement. It should be mentioned that the TN panel we employed was not a perfect broadband half-wave plate for all the visible light, which was optimized for a green light. As a result, the outgoing beam after PML is not circularly polarized for some wavelengths. This factor also degrades the CR improvement for white light input,

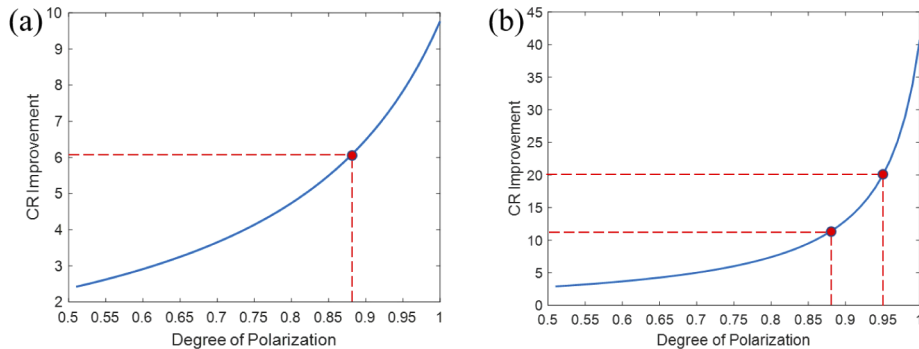


Fig. 8. Contrast ratio improvement of the proposed HUD system for dark state (a) without antireflection film and (b) with antireflection film.

which is about 3x in our experiment. Since the employed TN panel is optimized for the green wavelength, in experiment we let the display light incident from the green layer side of our CLC optical combiner, which helps slightly to improve the contrast ratio.

4. Discussion

Currently, the ambient light transmittance of our device is less than 70%. To achieve a higher ambient light transmittance, we can narrow the CLC reflection bands to better match the wavelength spectrum of the display, while preserving the polarization selectivity and wavelength selectivity. Hence, the display light reflection will be more efficient. If the reflection band is very narrow and sharp at the RGB primary colors of the display panel, then it can achieve higher R and T , becoming more similar to conventional holographic OCs.

The reflection bandwidth of a CLC film is related to the birefringence (Δn) of the employed LC material and the CLC helical pitch length (p) as $\Delta\lambda = p \cdot \Delta n$ [28]. By using a lower Δn LC, the reflection band gets narrower. Currently, the material we used is RM257, whose $\Delta n \approx 0.16$ in the green spectrum. DIC's UCL001 has a much lower birefringence ($\Delta n = 0.08$). If we use UCL001 to replace RM257 and fabricate the three-layer CLC film, the simulated Bragg reflection bands are plotted in Fig. 9(a). Consequently, the corresponding reflection spectrum of display light and the transmission spectrum of ambient light are shown in Figs. 9(b) and 9(c). Through integrating the area covered by red line and then divided by the area covered by blue line in Fig. 9(c) and Fig. 9(b), we find the ambient light transmittance is 78.9% and the display light reflectance is 70.5%, respectively.

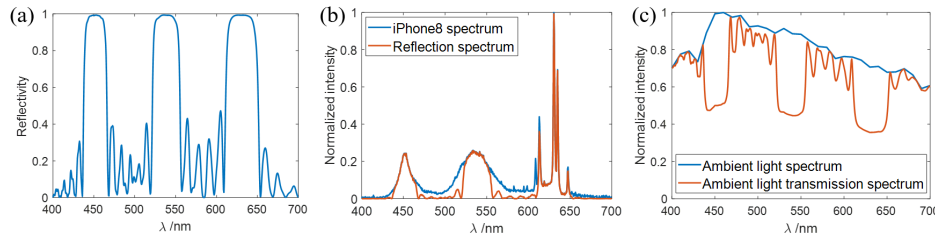


Fig. 9. (a) Reflection spectrum of narrowband three-layer CLC OC with LCP input, (b) original and reflection spectrum of the display with narrowband CLC OC, (c) original and transmission spectrum of ambient light with narrowband CLC OC.

The color shifts caused by the polarization selective OC can also be evaluated. Since the driver observes the virtual image reflected by the CLC OC and the real-world image transmitted through the CLC optical combiner, the color performance is assessed based on the display reflection spectrum [Fig. 6(a) and Fig. 9(b)] and ambient light transmission spectrum [Fig. 6(b) and Fig. 9(c)]. In Fig. 10, we plot the white points of the display, ambient light, reflection, and transmission spectrums in CIE 1976 color space. For the display image reflection spectrum, the color shift value $\Delta u'v'$ of broadband and narrowband CLC OC is 0.0014 and 0.0098, respectively. For the ambient light transmission spectrum, the color shift value of broadband and narrowband CLC combiner is 0.0107 and 0.0026, respectively. All the color shifts remain below 0.02 and are acceptable for commercial applications [29]. Moreover, in considering the eyepoint shifting, we also measured the shifted display reflection spectrum of our broadband CLC combiner. When the viewing angle shifts 15° , the color shift $\Delta u'v'$ increases from 0.0063 to 0.01, which is still below the indistinguishable level (0.02). The reason this eyepoint shifting will not cause too much color shift is that our three-layer CLC film is a broadband device. Even if the reflection band shifts slightly, it still covers the RGB primary colors of the display. As a result, the reflection spectrum will not change too noticeably.

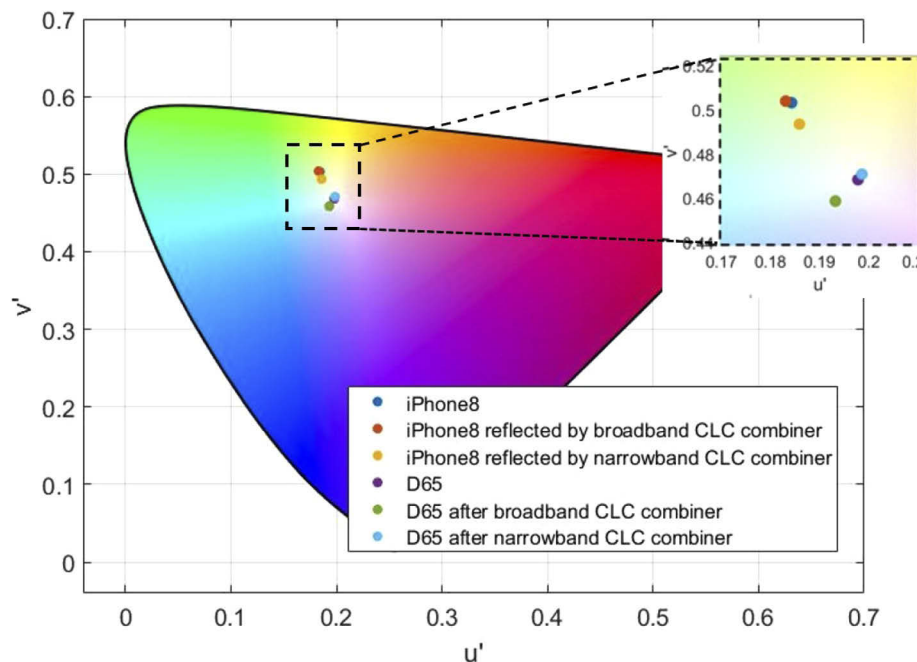


Fig. 10. White points of the display, ambient light, reflection, and transmission spectrums in CIE 1976 color space. D65: Ambient light.

5. Conclusion

In conclusion, we demonstrate a high dynamic range HUD to overcome the image washout and light leakage problems. The reported system utilizes a three-layer CLC film as the optical combiner, which is fabricated by a simple method. Based on the polarization selectivity of the CLC film, the polarization states of image content area pixels and blank area pixels are converted to LCP and RCP, respectively, by the PML. Both the bright state and dark state performances are improved, and the measured CR is enhanced by 7.5x, which corresponds to an 8.75dB dynamic range improvement. No noticeable color shift on the display reflection spectrum and ambient light transmission spectrum is observed. All the elements we utilized are cost effective and easily available. Potential applications of the proposed system for advanced HUDs are foreseeable.

Funding

a.u.Vista, Inc.

Disclosures

The authors declare no conflicts of interest.

References

1. J. M. Naish, "A system for presenting steering information during visual flight (the head-up display): Part 1: the effect of location of the instrument display on combined instrument and visual flying," <http://resolver.tudelft.nl/uuid:30549a4c-69a4-4674-8e3b-5ce51bf41aed>.
2. M. Weihrauch, G. Meloeny, and T. Goesch, "The First Head Up Display Introduced by General Motors," SAE Technical Paper 890288, (1989). <https://doi.org/10.4271/890288>.
3. Y. C. Liu and M. H. Wen, "Comparison of head-up display (HUD) vs. head-down display (HDD): driving performance of commercial vehicle operators in Taiwan," *Int. J. Man-Mach. Stud.* **61**(5), 679–697 (2004).

4. M. Tonnis, C. Lange, and G. Klinker, "Visual longitudinal and lateral driving assistance in the head-up display of cars," *IEEE and ACM International Symposium on Mixed and Augmented Reality* (IEEE, 2007), pp. 91–94.
5. C. R. Spitzer, U. Ferrell, and T. Ferrell, *Digital Avionics Handbook* (Taylor & Francis, 2014), Chap. 17.
6. T. Zhan, Y. H. Lee, J. Xiong, G. Tan, K. Yin, J. Yang, S. Liu, and S. T. Wu, "High-efficiency switchable optical elements for advanced head-up displays," *J. Soc. Inf. Disp.* **27**(4), 223–231 (2019).
7. H. Chen, G. Tan, M. Li, S. L. Lee, and S. T. Wu, "Depolarization effect in liquid crystal displays," *Opt. Express* **25**(10), 11315–11328 (2017).
8. Renesas white paper, "Implementing Laser Scanned-MEMS Projection in Automotive Head-Up Displays" (Renesas Electronics, 2018). <https://www.renesas.com/us/en/doc/whitepapers/optoelectronics/laser-scanned-mems-automotive-hud.pdf>.
9. K. Blankenbach, R. Isele, D. Stindt, and E. Buckley, "Comparison of the Readability of Colour Head-up Displays Using LED and Laser Light Sources," *Dig. Tech. Pap. - Soc. Inf. Disp. Int. Symp.* **41**(1), 1426–1429 (2010).
10. Y. Huang, G. Tan, F. Gou, M. C. Li, S. L. Lee, and S. T. Wu, "Prospects and challenges of mini-LED and micro-LED displays," *J. Soc. Inf. Disp.* **27**(7), 387–401 (2019).
11. J. Nakagawa, H. Yamaguchi, and T. Yasuda, "Head up display with laser scanning unit," *Proc. SPIE* **11125**, 12 (2019).
12. B. Ballard, V. Bhakta, M. Douglass, P. Gelabert, J. Kempf, W. McDonald, G. Pettitt, P. Rancuret, A. Rankin, J. Thompson, and P. I. Oden, "'Steering' Light with Texas Instruments Digital Micromirror Device (DMD)-Past, Present & Future," *Dig. Tech. Pap. - Soc. Inf. Disp. Int. Symp.* **47**(1), 28–31 (2016).
13. M. O. Freeman, "MEMS scanned laser head-up display," *Proc. SPIE* **7930**, 79300G (2011).
14. F. Rui, X. Zhang, and Z. Tu, "Influence of ambient temperature on OLED lifetime and uniformity based on modified equivalent lifetime detection," *J. Soc. Inf. Disp.* **27**(10), 597–607 (2019).
15. G. Tan, Y. Huang, M. C. Li, S. L. Lee, and S. T. Wu, "High dynamic range liquid crystal displays with a mini-LED backlight," *Opt. Express* **26**(13), 16572–16584 (2018).
16. A. Paranjpe, J. Montgomery, and S. M. Lee, "Manufacturing Solutions for Micro-LED Displays," *Dig. Tech. Pap. - Soc. Inf. Disp. Int. Symp.* **50**(S1), 169–172 (2019).
17. Y. Huang, E. L. Hsiang, M. Y. Deng, and S. T. Wu, "Mini-LED, Micro-LED and OLED displays: Present status and future perspectives," *Light: Sci. Appl.* **9**(1), 105 (2020).
18. Y. Ohe, M. Kume, Y. Demachi, T. Taguchi, and K. Ichimura, "Application of a novel photopolymer to a holographic head-up display," *Polym. Adv. Technol.* **10**(9), 544–553 (1999).
19. P. Coni, N. Damamme, and J. L. Bardon, "The Future of Holographic Head-Up Display," *IEEE Consumer Electron. Mag.* **8**(5), 68–73 (2019).
20. H. Chen, J. H. Lee, B. Lin, S. Chen, and S. T. Wu, "Liquid crystal display and organic light-emitting diode display: present status and future perspectives," *Light: Sci. Appl.* **7**(3), 17168 (2018).
21. M. F. Weber, A. J. Onderkirk, J. A. Wheatley, and J. Brodd, "Head-up display with polarized light source and wide-angle p-polarization reflective polarizer," U. S. patent 6,952,312 (Oct 4, 2005).
22. A. L. Berman, "Heads-up display combiner utilizing a cholesteric liquid crystal element," U. S. patent 4,900,133 (Feb 13, 1990).
23. N. Y. Ha, Y. Ohtsuka, S. M. Jeong, S. Nishimura, G. Suzuki, Y. Takanishi, K. Ishikawa, and H. Takezoe, "Fabrication of a simultaneous red-green-blue reflector using single-pitched cholesteric liquid crystals," *Nat. Mater.* **7**(1), 43–47 (2008).
24. Y. Huang, Y. Zhou, and S. T. Wu, "Broadband circular polarizer using stacked chiral polymer films," *Opt. Express* **15**(10), 6414–6419 (2007).
25. M. Schadt and W. Helfrich, "Voltage-dependent optical activity of a twisted nematic liquid crystal," *Appl. Phys. Lett.* **18**(4), 127–128 (1971).
26. H. Ren, S. Xu, Y. Liu, and S. T. Wu, "Switchable focus using a polymeric lenticular microlens array and a polarization rotator," *Opt. Express* **21**(7), 7916–7925 (2013).
27. W. D. St. John, W. J. Fritz, Z. J. Lu, and D. K. Yang, "Bragg reflection from cholesteric liquid crystals," *Phys. Rev. E: Stat. Phys., Plasmas, Fluids, Relat. Interdiscip. Top.* **51**(2), 1191–1198 (1995).
28. M. Mitov, "Cholesteric liquid crystals with a broad light reflection band," *Adv. Mater.* **24**(47), 6260–6276 (2012).
29. Y. L. Chen, J. C. Hsiang, Y. H. Wu, and C. L. Yang, "Multi-domain fringe-field switched mobile LCD for reducing color shift by zigzag-like pixel design," *Dig. Tech. Pap. - Soc. Inf. Disp. Int. Symp.* **41**(1), 1709–1712 (2010).